LANGMUIR

Article

pubs.acs.org/Langmuir

Thermoswitchable Janus Gold Nanoparticles with Stimuli-Responsive Hydrophilic Polymer Brushes

Xiaoqin Niu,[†] Fen Ran,*[,†,‡] Limei Chen,[†] Gabriella Jia-En Lu,[†] Peiguang Hu,[†] Christopher P. Deming,[†] Yi Peng,[†] Mauricio D. Rojas-Andrade,[†] and Shaowei Chen*[,†]

[†]Department of Chemistry and Biochemistry, University of California, 1156 High Street, Santa Cruz, California 95064, United States

[‡]State Key Laboratory of Advanced Processing and Recycling of Non-ferrous Metals, Lanzhou University of Technology, Lanzhou 730050, P. R. China

Supporting Information

ABSTRACT: Well-defined thermoswitchable Janus gold nanoparticles with stimuli-responsive hydrophilic polymer brushes were fabricated by combining ligand exchange reactions and the Langmuir technique. Stimuli-responsive polydi(ethylene glycol) methyl ether methacrylate was prepared by addition−fragmentation chain-transfer polymerization. The polymer brushes were then anchored onto the nanoparticle surface by interfacial ligand exchange reactions with hexanethiolate-protected gold nanoparticles, leading to the formation of a hydrophilic (polymer) hemisphere and a hydrophobic (hexanethiolate) one. The resulting Janus nanoparticles showed temperature-switchable wettability, hydrophobicity at high temperatures, and hydrophilicity at low temperatures, due to thermally induced conformational transition of the polymer ligands. The results further highlight the importance of interfacial engineering in the deliberate functionalization of nanoparticle materials.

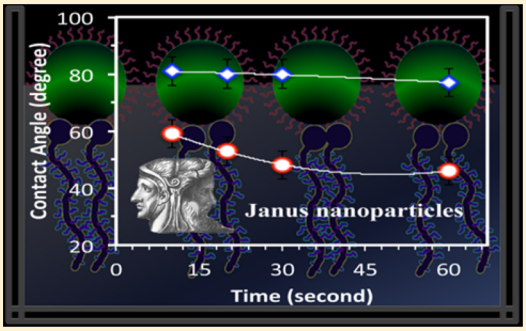

1. INTRODUCTION

Nanometer-sized metal particles have been attracting significant attention primarily due to their unique chemical and physical properties that deviate significantly from those of their constituent atoms and bulk forms.[1−3] Janus nanoparticles, analogous to the Janus god in ancient Roman mythology, represent a unique family of functional materials that exhibit an asymmetrical structure, such as two hemispheres of different shapes, chemical compositions, and/or surface functionality.[4−9] Such structural asymmetry may serve as a new, effective parameter in the manipulation of the nanoparticle physical/chemical properties by, for instance, directional functionalization and controlled assembly.[10] There have been a variety of methods reported in the literature toward the synthesis of Janus nanoparticles, e.g., the template method, Pickering emulsion method, interfacial method, the "grafting to" approach, etc.[11−14] Of these, interfacial engineering based on the Langmuir method represents an effective procedure,[15,16] where hydrophobic alkanethiolate-passivated metal nanoparticles are exploited as the initial starting materials and undergo ligand exchange reactions with hydrophilic thiol ligands on the water surface of a Langmuir−Blodgett trough.[17,18] Yet, thus far, in the obtained Janus nanoparticles, both the hydrophilic and hydrophobic ligands have been limited to relatively simple molecules, and the scope of manipulation of the nanoparticle structures and properties remains rather narrow.[19] One may ask, is it possible to incorporate macromolecular chains onto the Janus nanoparticle surface where the rich chemistry of polymers may then be exploited for further functionalization of the nanoparticles? It is within this context that this study was carried out.

Preparation of polymer-tethered nanoparticles has been described in a number of recent studies.[20−24] However, studies on the fabrication of polymer-capped Janus nanoparticles have remained relatively scarce. For instance, Kim et al. studied the phase behaviors of mixed polymers of polystyrene and poly(methyl methacrylate) anchored on gold nanoparticle surface by small-angle neutron scattering, and observed phase segregation of the two polymers which resulted in the formation of Janus-type nanoparticles.[25] Recently, Percebom et al. also prepare Janus gold nanoparticles by exploiting spontaneous segregation of two immiscible polymers on the nanoparticle surface.[26] In another study, Li et al. prepared Janus gold nanoparticles by incorporating polystyrene onto the nanoparticle surface by one-step reverse atom transfer radical polymerization in emulsion as well as by a facile spontaneous assembly method at the liquid−liquid interface.[27,28] Alternatively, Wang et al. synthesized Janus gold nanoparticles with two different polymers, poly(ethylene oxide) and poly(methyl methacrylate)/poly(*t*-butyl acrylate), on the opposite hemispheres of the nanoparticles by integration of the "solid-state grafting-to" and "grafting-from" methods, using single-crystalline templates based on various polymers (e.g., polyethylene, nylon, and polypeptides).[29] Despite the progress, much remains

Received: February 13, 2016
Revised: March 31, 2016
Published: April 11, 2016

DOI: 10.1021/acs.langmuir.6b00562
Langmuir 2016, 32, 4297−4304

to be done, in particular, in the functionalization of Janus nanoparticles with thermoresponsive polymers.

Notably, a number of smart materials have been prepared based on thermoresponsive polymers that exhibit a lower critical solution temperature (LCST) or an upper critical solution temperature (UCST) in water, and may be used for diverse applications, for instance, chemical/biological sensing, tissue engineering, and drug delivery.[30−32] Of these, oligo(ethylene glycol) methacrylates (OEGMAs), which may be prepared by various effective methods such as atom transfer radical polymerization and reversible addition−fragmentation chain-transfer polymerization, exhibit interesting stimuli-responsive characteristics.[33,34] Significantly, OEGMA-based polymers can be readily anchored onto a wide variety of substrates, ranging from flat surfaces to porous networks, and colloidal particles,[35] and various synthetic OEGMA-based polymers, for instance, 2-(2-methoxyethoy)ethyl methacrylate (MEO_2MA), MEO_3MA, $OEGMA_{300}$, and $OEGMA_{475}$,[36,37] have indeed been used to prepare polymer tethered nanoparticles. Yet in these prior studies, there is virtually no spatial control of the tethering of the polymer chains onto the nanoparticle surface.

Herein, we described an effective procedure to prepare thermoswitchable Janus gold nanoparticles with stimuli-responsive OEGMA polymer brushes. Experimentally, reversible addition−fragmentation chain-transfer (RAFT) polymerization was employed to synthesize polydi(ethylene glycol) methyl ether methacrylate, with a well-defined molecular weight, which was then utilized as hydrophilic ligands to prepare Janus gold nanoparticles by interfacial ligand exchange reactions. It was found that the resulting Janus nanoparticles exhibited apparent temperature-switchable wettability property: hydrophobic at high temperatures and hydrophilic at low temperatures.

2. EXPERIMENTAL SECTION

2.1. Chemicals. Di(ethylene glycol) methyl ether methacrylate (MEO_2MA, 95%), cyanomethyl dithiobenzoate (CMTB, 98%), azodiisobutyronitrile (AIBN) and *n*-butylamine were purchased from Sigma-Aldrich. MEO_2MA were distilled under vacuum and AIBN was recrystallized from ethanol prior to use. Solvents were purchased from typical commercial sources at their highest purity and used without further treatment. Water was supplied by a Barnstead Nanopure water system (18.3 MΩ cm).

2.2. Synthesis of Polydi(ethylene glycol) Methyl Ether Methacrylate Terminated with the RAFT Agent ($PMEO_2MA$-CMTB). $PMEO_2MA$-CMTB was synthesized by RAFT polymerization, as described previously.[38,39] In a typical reaction, MEO_2MA (0.6 g, 3.2 mmol), CMTB (0.02 g, 0.1 mmol), and AIBN (0.004 g) were dissolved in 4 mL of anisole in a 15 mL flask to form a homogeneous solution under magnetic stirring (corresponding to a MEO_2MA/CMTB mass ratio of 30:1). Then, the mixture was degassed under vacuum for 10 min and refilled with nitrogen for three times. After that, polymerization was carried out in an oil bath at 60 °C for 24 h before the reaction solution was cooled down to room temperature. $PMEO_2MA$-CMTB was obtained by precipitation in cold pentane for three times and dried under vacuum for 24 h. Three additional polymers were prepared in a similar fashion but at different monomer to RAFT agent mass ratios, 10:1, 60:1, and 150:1. The corresponding molecular weights and polydispersity indexes are included in Table S1 in the Supporting Information.

2.3. Synthesis of Thiol-Ended $PMEO_2MA$ ($PMEO_2MA$-SH). To prepare thiol-terminated polymer macromolecules, dithioester-terminated $PMEO_2MA$ was reduced by *n*-butylamine in THF. In a typical reaction, $PMEO_2MA$-CMTB prepared above (1 g, 0.02 mmol) was dissolved in 20 mL of THF, and *n*-butylamine (80 mg, 1.1 mmol) was added under magnetic stirring and nitrogen. After 2 h, the polymer was precipitated in cold pentane for three times and dried under vacuum for 24 h, affording $PMEO_2MA$-SH.

2.4. Fabrication of Gold Janus Nanoparticles. 1-Hexanethiolate-protected gold nanoparticles (AuC6) were prepared and purified by using the Brust protocol.[40] The nanoparticles exhibited an average core diameter of 5.41 ± 0.80 nm, as determined by transmission electron microscopic measurements of more than 200 nanoparticles,[41] and used to prepare Janus nanoparticles.[42,43] Briefly, a monolayer of the AuC6 nanoparticles was first formed on the water surface of a Langmuir−Blodgett trough (NIMA Technology, model 611D) with the water temperature controlled at 8 °C. The particle monolayer was then compressed to a desired surface pressure where the interparticle separation was maintained at a value smaller than twice the extended ligand chain length such that the interfacial mobility of the particles was impeded. At this point, a calculated amount of a water solution of the $PMEO_2MA$−SH polymers prepared above (1 mg/mL in water at 8 °C) was injected into the water subphase by using a Hamilton microliter syringe. After 6 h of interfacial ligand exchange reactions, the resulting Janus nanoparticles were transferred onto a clean glass slide surface, rinsed with cold water three times, and dispersed in THF.

2.5. Characterizations of Polymers and Gold Nanoparticles. The number-average molecular weight of the copolymer was determined by using gel permeation chromatography (GPC) with an HP1100 using two PL gel columns with monodisperse polystyrene as the standard. The mobile phase was THF, the sample concentration was 1.0 g/L, the detector was an RID, and the flow rate was 1.0 mL/min. FTIR measurements were carried out with a PerkinElmer FTIR spectrometer (Spectrum One, spectral resolution 4 cm^{-1}) where the samples were prepared by casting the polymer or particle solutions onto a ZnSe disk. ^1H NMR spectra were recorded on a Varian Unity Plus 300/54 NMR spectrometer using chloroform-*d* as the solvent. UV−vis absorption spectra were collected with a PerkinElmer Lambda 35 UV−vis spectrometer by using a 1 cm quartz cuvette. X-ray photoelectron (XPS) spectra were recorded with a PHI 5400/XPS instrument equipped with an Al Kα source operated at 350 W and 10^{-9} Torr. Silicon wafers were sputtered by argon ions to remove carbon from the background and used as substrates. Dynamic light scattering (DLS) studies were carried out by using a Wyatt DynaPro NanoStar temperature-controlled microsampler with the nanoparticles dissolved in selected solvents. An aliquot (5 μL) of the particle solutions at a concentration of ca. 0.05 mg/mL was introduced into a sample holder by using a 10 μL micropipet. Data were acquired at different temperatures, and results were reported in terms of mass %. Contact angles were measured with a Tantec CAM-PLUS contact angle meter. Experimentally, the Janus nanoparticle monolayers were transferred onto a clean glass slide surface (3 cm × 8 cm) from the water surface by either the upstroke or downstroke deposition method, and dried under vacuum for 24 h. Control experiments were also carried out where pristine polymer films were prepared by drop-casting a polymer dispersion onto a glass slide surface and dried in a vacuum oven.[44] For each sample, measurements were carried out at both room temperature (about 28 °C) and lower temperature (about 8 °C), and at least eight independent measurements were carried out for statistical analyses.

3. RESULTS AND DISCUSSION

3.1. Syntheses and Characterization of PEO_2MA−SH. The synthetic procedure of $PMEO_2MA$−SH is summarized in Scheme 1. RAFT polymerization was used to synthesize polydi(ethylene glycol) methyl ether methacrylate where the RAFT agent group was attached onto the molecular terminal ($PMEO_2MA$−CMTB). From GPC measurements using polystyrene standards, the mean molecular weight (M_n) of the $PMEO_2MA$−CMTB polymers was found to increase with increasing monomer/RAFT agent mass ratio, 1500 g/mol at 10:1, 4800 g/mol at 30:1, 10 200 g/mol at 60:1, and 30 400 g/mol at 150:1, whereas the polydispersity index (PDI, M_w/M_n)

DOI: 10.1021/acs.langmuir.6b00562
Langmuir 2016, 32, 4297−4304

Scheme 1. Synthetic Procedure of $PMEO_2MA-SH$

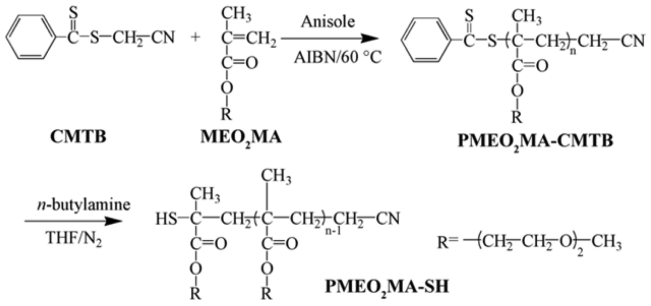

remained virtually unchanged at 1.2−1.3 (Table S1). The narrow distribution of the molecular weight of each sample was ascribed to the rational RAFT agent for the monomer. Finally, excess *n*-butylamine was added under magnetic stirring in a nitrogen atmosphere to reduce $PMEO_2MA-CMTB$ to thiol-ended polymer ($PMEO_2MA-SH$). In the present study, we would focus on the polymer of M_n = 4800 g/mol, as it exhibited the optimal molecular weight in the preparation of Janus nanoparticles (vide infra).

Spectroscopic measurements were then carried out to characterize the structures of the obtained polymers. From the FTIR spectra in Figure 1, one can see several vibrational

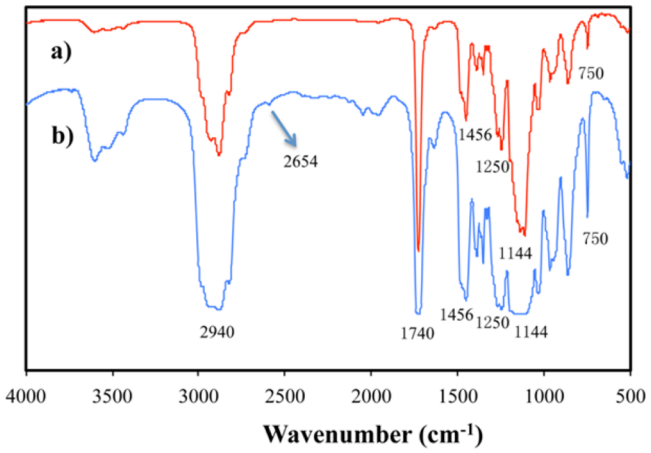

Figure 1. FTIR spectra of (a) $PMEO_2MA-CMTB$ and (b) $PMEO_2MA-SH$.

bands that were characteristic of $PMEO_2MA$ for (a) $PMEO_2MA-CMTB$ and (b) $PMEO_2MA-SH$: methyl and methylene C−H stretches at 2940 cm^{-1}, C═O stretch at 1740 cm^{-1}, CH_2 bending at 1456 cm^{-1}, and CH_2-O stretching at 1150−1070 cm^{-1}. Yet, there is a noticeable difference between $PMEO_2MA-CMTB$ and $PMEO_2MA-SH$, where a new weak band appeared at 2654 cm^{-1} in $PMEO_2MA-SH$, most likely due to the terminal S−H group (additional data in Table S2). Consistent results were obtained in ^1H NMR measurements, which further confirmed the successful synthesis of the polymers. Figure 2 shows the ^1H NMR spectra of (a) $PMEO_2MA-CMTB$ and (b) $PMEO_2MA-SH$ in chloroform-*d*, which were rather consistent at δ 0.79−1.09 ppm (3H, CH_3-C-), δ 1.61−2.02 ppm (2H, $-C-CH_2-C$), δ 3.37−3.41 ppm (3H, CH_3-O-), δ 3.52−3.79 ppm (2H, $-CH_2-O-$), and δ 4.04−4.18 ppm (2H, $-CH_2-O-CO-$). Yet, there is a marked difference. One can see that $PMEO_2MA-CMTB$ also exhibited multiple weak peaks within the range of δ 7.47−8.15

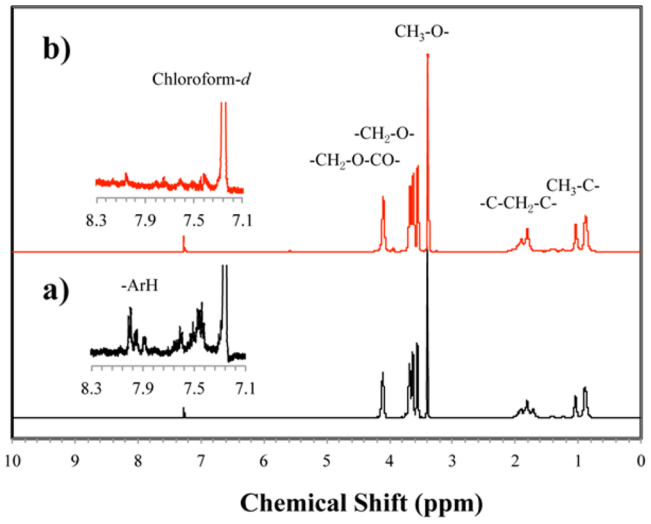

Figure 2. ^1H NMR spectra of (a) $PMEO_2MA-CMTB$ and (b) $PMEO_2MA-SH$. Insets show the zoom-in of the respective region between 7.1 and 8.3 ppm.

ppm (inset to panel a), which likely arose from the aromatic terminus of the RAFT agent (Scheme 1). These peaks disappeared almost completely in $PMEO_2MA-SH$ (inset to panel b), suggesting effective removal of the aromatic rings and the successful transformation of the thiolester group to thiol moiety.

UV−vis measurements were also carried out to provide further insights into the structural evolution of $PMEO_2MA$. The absorption profiles of $PMEO_2MA-CMTB$ and $PMEO_2MA-SH$ in THF were depicted in Figure 3. It can be seen that $PMEO_2MA-CMTB$ exhibited an exponential decay profile with an absorption peak at 310 nm, characteristic of the −CMTB group in the polymer, which vanished completely after chemical reduction of dithioester in the formation of $PMEO_2MA-SH$. Experimentally, the reduction of dithioester

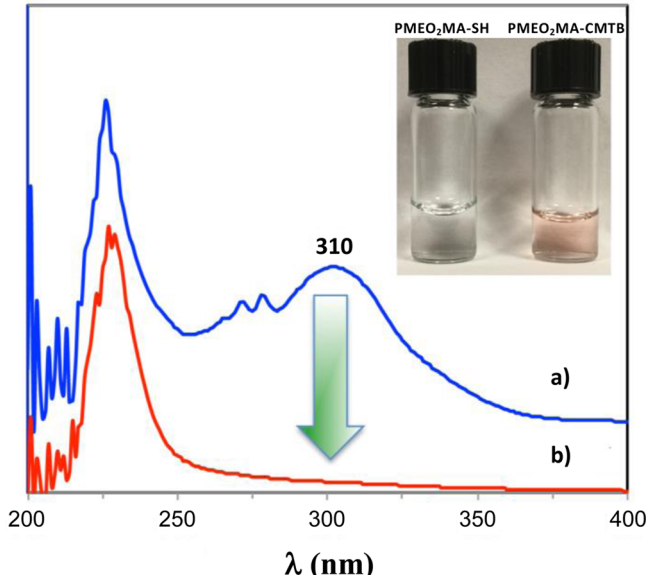

Figure 3. UV−vis spectra of (a) $PMEO_2MA-CMTB$ and (b) $PMEO_2MA-SH$ in THF. Inset is a photograph of the two polymer solutions.

DOI: 10.1021/acs.langmuir.6b00562
Langmuir 2016, 32, 4297−4304

to thiol also led to an apparent color change from light red to colorless of the polymer solution in THF (inset to Figure 3).

3.2. Preparation and Characterization of Polymer-Capped Gold Nanoparticles. Gold Janus nanoparticles with $PMEO_2MA-SH$ as the hydrophilic ligands were prepared by using a procedure based on the Langmuir method that we developed previously (Figure 4 left panels).[43] It should be noted that $PMEO_2MA-SH$, as mentioned above, is a kind of OEGMA-based polymers and exhibits an LCST in water of ca. 10–15 °C,[30,31] so the water temperature must be set below LCST to ensure effective dissolution in water. In fact, at decreasing temperature we observed that $PMEO_2MA-SH$ was initially insoluble in water at 28 °C, became turbid at 18 °C, and was totally soluble at 8 °C; and the observations might be reversed by increasing the water temperature, as manifested in the right panels of Figure 4 (0.1 g of $PMEO_2MA-SH$ in 20 mL of water). Thus, experimentally, to ensure good solubility of the polymer in water, the Janus nanoparticles were prepared by controlling the temperature of the water subphase at 8 °C.

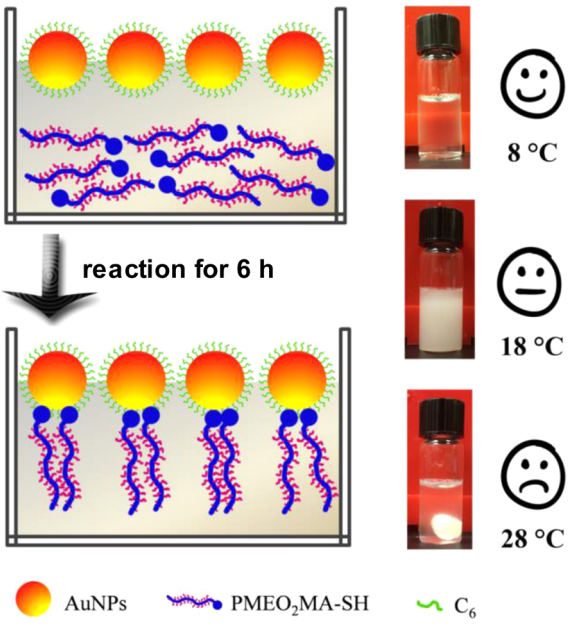

Figure 4. (Rigth) Photographs of a polymer solution at different temperatures (0.1 g of $PMEO_2MA-SH$ in 20 mL of water) and (left) schematic illustrations for preparation of $PMEO_2MA$-tethered gold Janus nanoparticles at 8 °C.

Note that in the above procedure for the formation of Janus nanoparticles, the nanoparticles were confined at the air|water interface.[43] We found that it was important to use polymers of proper molecular weights (M_n), because if M_n was too high, the nanoparticles might be pulled into the water subphase after tethering of the polymer chains onto the nanoparticle surface. This would destroy the structural integrity of the nanoparticle monolayer and hence the quality of the Janus structure. In fact, of the four $PMEO_2MA-SH$s synthesized (Table S1), we found that the two smaller polymers (M_n = 1500 and 4800 g/mol) were more efficient in the fabrication of Janus nanoparticles than the two larger ones (10 200 and 30 400 g/mol). Experimentally, during the interfacial ligand exchange reaction, small M_n polymers-tethered gold nanoparticles remained on the water surface retaining the same monolayer structure (as monitored by surface pressure), whereas when high M_n polymers were used instead, it became visible by naked eyes that a number of holes (several mm in diameter) were formed within the nanoparticle films, apparently because part of the polymer-tethered nanoparticles were submersed into the water subphase. Thus, in the present study, we focus on Janus nanoparticles that were prepared with $PMEO_2MA-SH$ (4800 g/mol).

The Janus nanoparticles were then collected from the water surface, transferred into a THF solution, and centrifuged to remove loosely bound polymer macromolecules, as manifested by UV–vis measurement where the residual concentration of $PMEO_2MA-SH$ in the supernatant after centrifugation was estimated below 10^{-9} mg/mL. The structure of the obtained Janus nanoparticles was then characterized, in comaprison with that of the original AuC6 nanoparticles. From the FTIR spectra in Figure 5, one can see that the polymer-capped gold Janus nanoparticles exhibited the same vibrational features charateristic of $PMEO_2MA$ (Figure 1), with clearly defined bands at 2940, 1740, 1456, and 1150–1070 cm^{-1}, confirming the successful tethering of the polymer chains onto the nanoparticle surface (summarized in Table S3).

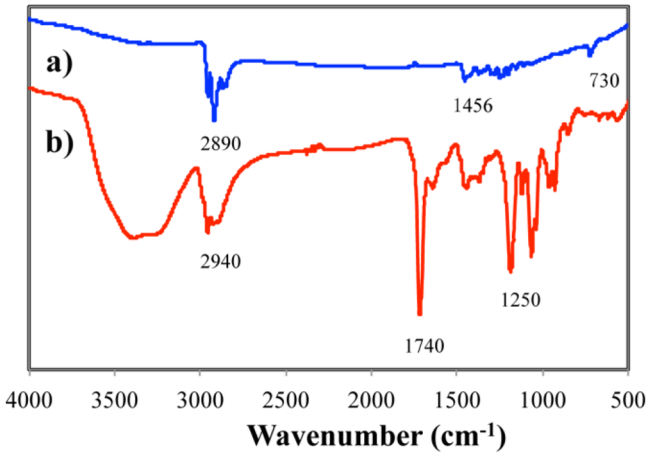

Figure 5. FTIR spectra for (a) AuC6, and (b) $PMEO_2MA$-tethered gold Janus nanoparticles.

Further structural insights were obtained in ^1H NMR and XPS measurements. From the ^1H NMR spectrum in Figure 6, one can see that the spectral features were consistent with those of $PMEO_2MA$ in Figure 2, i.e., δ 0.79–1.09 ppm (3H, CH_3–C–), δ 1.61–2.02 ppm (2H, –C–CH_2–C), δ 3.37–3.41 ppm

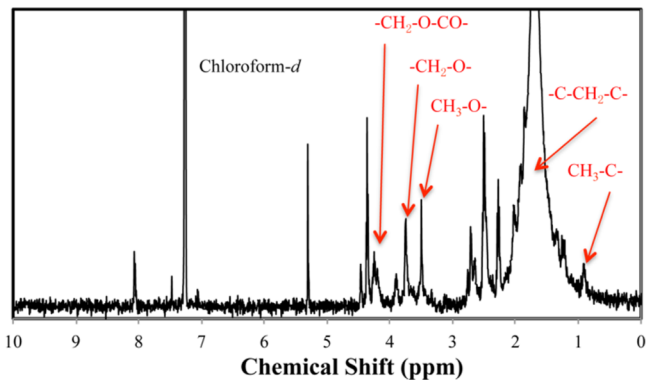

Figure 6. ^1H NMR spectrum for $PMEO_2MA$-tethered gold Janus nanoparticles in $CDCl_3$.

DOI: 10.1021/acs.langmuir.6b00562
Langmuir 2016, 32, 4297–4304

(3H, CH_3−O−), δ 3.52−3.79 ppm (2H, −CH_2−O−), and δ 4.04−4.18 ppm (2H, −CH_2−O−CO−). In addition, based on the integrated peak areas, the ratio of the methyl protons at δ = 3.37−3.41 ppm (CH_3−O−) to those at δ = 0.79−1.09 ppm (CH_3−C−) was calculated to be 1:1.2, corresponding to a molar ratio of 3:20 between the polymer chains and the original hexanethiolate ligands.

In XPS measurements of the polymer-capped gold Janus nanoparticles, the Au 4f, O 1s, C 1s, and S 2p electrons can be readily identified at ca. 84, 532, 286, and 163 eV, respectively, as manifested in the syurvey spectrum (Figure 7a). Figure 7b depicts the high-resolution scan of the C 1s electrons, where deconvolution yields five subpeaks at 284.6, 285.1, 286.2, 287.1, and 288.9 eV, corresponding to the carbons in C−C/C−H, C−C−O, C−O, C−S, and O−(C═O)−, respectively. Furthermore, from the integrated peak areas, the atomic ratio of the carbons in the polymer main chains (C−C regular) to those in the side chains (with O) was estimated to be 4.5:3.5, consistent with the molecular structure in Scheme 1, and the ratio of the polymer chains to hexanethiolate ligands was estimated to be 3:22, very close to that obtained from ^{1}H NMR measurements (Figure 6).

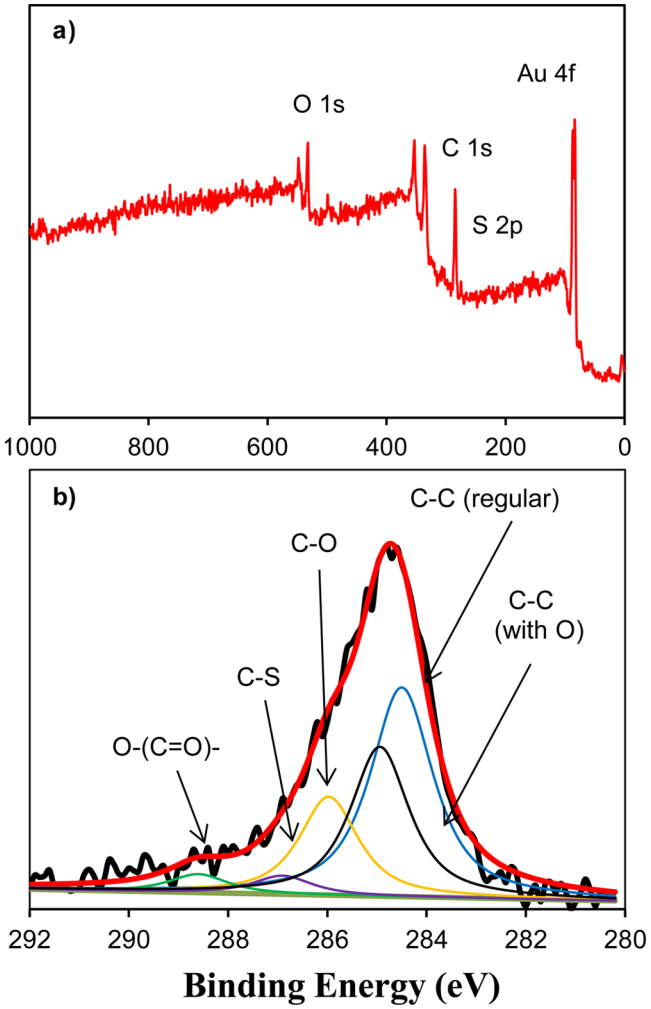

Figure 7. (a) XPS survey spectrum and (b) high-resolution scan of the C 1s electrons of the $PMEO_2MA$-tethered gold Janus nanoparticles.

Interestingly, the $PMEO_2MA$-tethered gold Janus nanoparticles exhibited apparent temperature-responsive wettability, as manifested by contact angle measurements. Experimentally, the Janus nanoparticles were transferred onto a clean glass slide surface by downstroke deposition and rinsed with cold water for six times to remove loosely bound polymers from the water subphase. In this deposition fashion, the hydrophobic (hexanethiolates) hemisphere of the nanoparticles was in direct contact with the glass slide, whereas the hydrophilic side (tethered polymers) was exposed (Figure 8 inset). We then measured the contact angles every 10 s within 1 min at 8 °C, and found that the contact angle decreased slowly from 60° at t = 10 s to 49° at t = 1 min (Figure 8). Notably, the results are very close to those of a drop-cast film of pristine $PMEO_2MA$ where the contact angles also exhibited a slow decrease from 46° at t = 10 s to 30° at t = 1 min, indicating a similarly hydrophilic surface of the two ensembles (the discrepancy of contact angles may be ascribed to the different surface roughness between these two thin films).

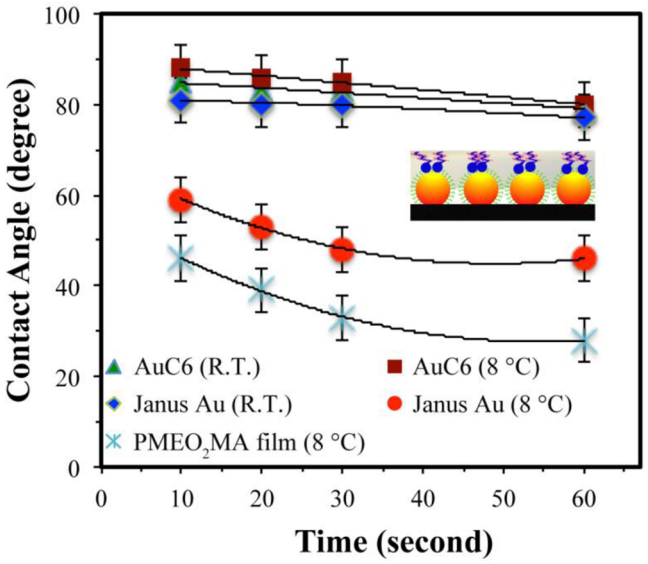

Figure 8. Contact angles of a Langmuir−Blodgett monolayer of AuC6 and $PMEO_2MA$-tethered gold Janus nanoparticles, and evaporated film of $PMEO_2MA$ at different temperatures.

More interestingly, when the contact angles of the Janus nanoparticle monolayer were measured at room temperature (ca. 28 °C), the results were markedly different. First, the contact angles were much higher than those acquired at 8 °C; second, the contact angles remained virtually invariant from 82° at t = 10 s to 80° at t = 1 min. This suggests that the nanoparticle surface became increasingly hydrophobic due to the tethered macromolecular ligand of $PMEO_2MA$. Note that as a temperature-sensitive polymer, $PMEO_2MA$ chains would strech out at low tempeatures (e.g., 8 °C) and show hydrophilic characters, but fold in at high temperatures (e.g., 28 °C) and display hydrophobic characters instead. This is consistent with the behaviors of the polymers in solution (Figure 4). Such temperatue-responsive behaviors could not be seen with the original AuC6 nanoparticles. In fact, from Figure 8, one can see that the contact angles for the original AuC6 nanoparticles were almost unchanged when the temperatured was increased from 8 to 28 °C. In addition, the contact angles for AuC6 nanoparticles at 8 °C were significantly higher than those of the $PMEO_2MA$-tethered Janus nanoparticles at the same temperature, but both the AuC6 and Janus nanoparticles

DOI: 10.1021/acs.langmuir.6b00562
Langmuir 2016, 32, 4297−4304

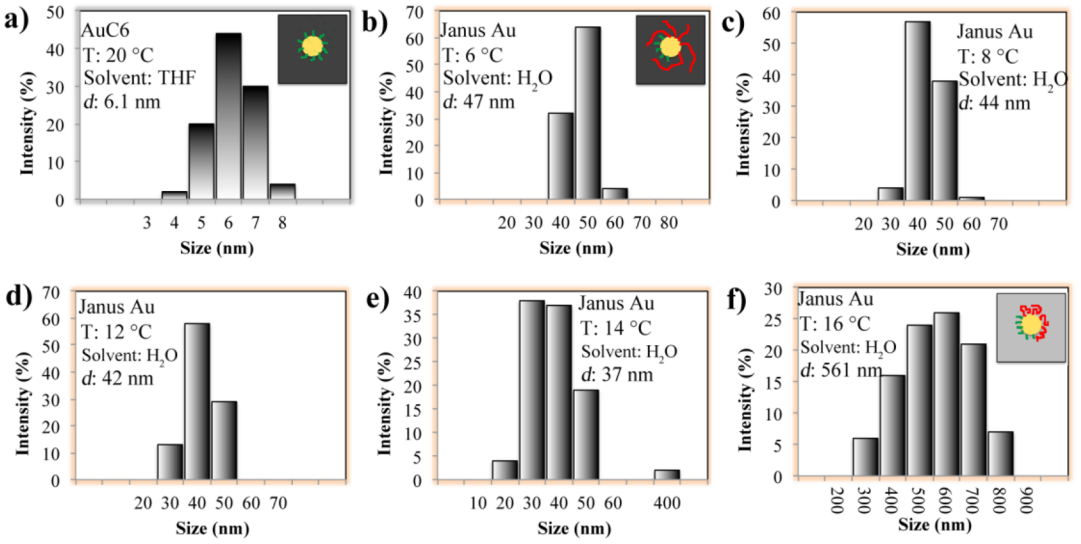

Figure 9. Distributions of hydrodynamic diameters determined by DLS measurements of AuC6 and $PMEO_2MA$-tethered Janus nanoparticles at different temperatures. Insets show the schematics of the ligand conformations of the corresponding nanoparticles.

exhibited almost identical contact angles at room temperature, suggesting that at this temperature both nanoparticles exposed a similarly hydrophobic surface. Furthermore, there is virtually no diminishment of the contact angles with time, suggesting a relatively stable surface structure.

The thermoresponsive properties were further probed by DLS measurements at controlled temperatures.[45] Figure 9 shows the distributions of the hydrodynamic diameters (D_H) of AuC6 and $PMEO_2MA$-tethered Janus nanoparticles determined by DLS measurements at different temperatures. For AuC6 nanoparticles in THF (panel a), the average diameter was estimated to be 6.1 nm at 20 °C, which remained virtually unchanged at lower temperatures (e.g., 6 °C, not shown). This indicates good dispersion of individual nanoparticles in THF. In contrast, the $PMEO_2MA$-tethered Janus nanoparticles in H_2O exhibited a much larger D_H, which was almost unchanged at ca. 40 nm within the temperature range of 6 to 14 °C (panels b–e). Yet, at higher temperatures (e.g., 16 °C, panel f), D_H showed a significant increase to 561 nm. This may be ascribed to the temperature-dependent conformational transition of the polymers tethered on the nanoparticle surface. At low temperatures, the macromolecular chains of $PMEO_2MA$ were likely fully stretched, which rendered the nanoparticles highly dispersible (well solvated) in water. Yet at high temperatures, because of contraction of the polymer chains and increasing hydrophobicity of the Janus nanoparticles (Figure 9), the solubility of the nanoparticlesin in water diminished such that the particles started to aggregate, as reflected by the large D_H. Taken together, these results indicate the successful preparation of well-defined thermoswitchable Janus gold nanoparticles with stimuli-responsive hydrophilic polymer brushes. This may be exploited as a new avenue for the rationale design and manipulation of nanoparticle structures and properties.

4. CONCLUSION

Thermosensitive polydi(ethylene glycol) methyl ether methacrylate was synthesized and used to prepared Janus gold nanoparticles by interfacial ligand-exchange reactions, as manifested by NMR, FTIR, and XPS measurements. Interestingly, contact angle measurements of monolayers of the Janus nanoparticles showed a marked increase with increasing temperature, due to the intrinsic thermoswitchable conformational transition of the polymer chains on the nanoparticle surface. In contrast, with the original AuC6 nanoparticles, virtually no change was observed. Consistent behaviors were seen in DLS measurements in water, where at temperatures below 14 °C the average hydrodynamic diameter was only ca. 40 nm, but at higher temperatures (≥16 °C) the hydrodynamic diameters increased by more than an order of magnitude, because of increasing hydrophobicity that drove the formation of large nanoparticle aggregates. The results further highlight the significance of nanoparticle surface functionalization with functional polymers in the further manipulation of nanoparticle materials properties.

■ ASSOCIATED CONTENT

Supporting Information

The Supporting Information is available free of charge on the ACS Publications website at DOI: 10.1021/acs.langmuir.6b00562.

Summary of molecular information on the four $PMEO_2MA$–CMTB polymers (PDF)

■ AUTHOR INFORMATION

Corresponding Authors

*E-mail: ranfen@163.com.
*E-mail: shaowei@ucsc.edu.

Author Contributions

The manuscript was written through contributions of all authors. All authors have given approval to the final version of the manuscript.

Notes

The authors declare no competing financial interest.

■ ACKNOWLEDGMENTS

This work was supported, in part, by grants from the National Science Foundation (CHE-1265635 and DMR-1409396). The authors also thank the Lawrence Berkeley National Laboratory, which is supported by the U.S. Department of Energy, for access to the XPS facilities at the Molecular Foundry.

DOI: 10.1021/acs.langmuir.6b00562
Langmuir 2016, 32, 4297–4304

REFERENCES

(1) Liu, K.; Zhao, N.; Kumacheva, E. Self-assembly of inorganic nanorods. *Chem. Soc. Rev.* **2011**, *40*, 656−671.
(2) Mokari, T.; Rothenberg, E.; Popov, I.; Costi, R.; Banin, U. Selective growth of metal tips onto semiconductor quantum rods and tetrapods. *Science* **2004**, *304*, 1787−1790.
(3) Jadzinsky, P. D.; Calero, G.; Ackerson, C. J.; Bushnell, D. A.; Kornberg, R. D. Structure of a thiol monolayer-protected gold nanoparticle at 1.1 Å resolution. *Science* **2007**, *318*, 430−433.
(4) Song, Y.; Chen, S. Janus Nanoparticles: Preparation, Characterization, and Applications. *Chem. - Asian J.* **2014**, *9*, 418−430.
(5) de Gennes, P. G. Soft matter. *Science* **1992**, *256*, 495−497.
(6) He, J.; Hourwitz, M. J.; Liu, Y.; Perez, M. T.; Nie, Z. One-pot facile synthesis of Janus particles with tailored shape and functionality. *Chem. Commun.* **2011**, *47*, 12450−12452.
(7) Cole-Hamilton, D. J. Janus Catalysts Direct Nanoparticle Reactivity. *Science* **2010**, *327*, 41−42.
(8) Loget, G.; Lee, T. C.; Taylor, R. W.; Mahajan, S.; Nicoletti, O.; Jones, S. T.; Coulston, R. J.; Lapeyre, V.; Garrigue, P.; Midgley, P. A.; Scherman, O. A.; Baumberg, J. J.; Kuhn, A. Direct Visualization of Symmetry Breaking During Janus Nanoparticle Formation. *Small* **2012**, *8*, 2698−2703.
(9) Jia, L.; Zhou, F.; Liu, W. M. Janus nanoparticle magic: selective asymmetric modification of Au-Ni nanoparticles for its controllable assembly onto attapulgite nanorods. *Chem. Commun.* **2012**, *48*, 12112−12114.
(10) Wurm, F.; Kilbinger, A. F. Polymeric janus particles. *Angew. Chem., Int. Ed.* **2009**, *48*, 8412−8421.
(11) Suzuki, D.; Tsuji, S.; Kawaguchi, H. Janus microgels prepared by surfactant-free pickering emulsion-based modification and their self-assembly. *J. Am. Chem. Soc.* **2007**, *129*, 8088−8089.
(12) Shah, R. K.; Kim, J. W.; Weitz, D. A. Janus supraparticles by induced phase separation of nanoparticles in droplets. *Adv. Mater.* **2009**, *21*, 1949−1953.
(13) Prasad, N.; Perumal, J.; Choi, C. H.; Lee, C. S.; Kim, D. P. Generation of monodisperse inorganic−organic janus microspheres in a microfluidic device. *Adv. Funct. Mater.* **2009**, *19*, 1656−1662.
(14) Maye, M. M.; Nykypanchuk, D.; Cuisinier, M.; van der Lelie, D.; Gang, O. Stepwise surface encoding for high-throughput assembly of nanoclusters. *Nat. Mater.* **2009**, *8*, 388−391.
(15) Pradhan, S.; Ghosh, D.; Chen, S. Janus nanostructures based on Au−TiO2 heterodimers and their photocatalytic activity in the oxidation of methanol. *ACS Appl. Mater. Interfaces* **2009**, *1*, 2060−2065.
(16) Xu, Q.; Kang, X.; Bogomolni, R. A.; Chen, S. Controlled assembly of Janus nanoparticles. *Langmuir* **2010**, *26*, 14923−14928.
(17) Fernandez-Rodriguez, M. A.; Song, Y.; Rodríguez-Valverde, M. A. n.; Chen, S.; Cabrerizo-Vilchez, M. A.; Hidalgo-Alvarez, R. Comparison of the interfacial activity between homogeneous and Janus gold nanoparticles by pendant drop tensiometry. *Langmuir* **2014**, *30*, 1799−1804.
(18) Song, Y.; Liu, K.; Chen, S. AgAu bimetallic Janus nanoparticles and their electrocatalytic activity for oxygen reduction in alkaline media. *Langmuir* **2012**, *28*, 17143−17152.
(19) Song, Y.; Chen, S. Janus Nanoparticles as Versatile Phase-Transfer Reagents. *Langmuir* **2014**, *30*, 6389−6397.
(20) Boyer, C.; Whittaker, M. R.; Luzon, M.; Davis, T. P. Design and synthesis of dual thermoresponsive and antifouling hybrid polymer/gold nanoparticles. *Macromolecules* **2009**, *42*, 6917−6926.
(21) Dong, J.; Zhou, J. Solvent-Responsive Behavior of Polymer-Brush-Modified Amphiphilic Gold Nanoparticles. *Macromol. Theory Simul.* **2013**, *22*, 174−186.
(22) Walther, A.; Müller, A. H. Janus particles: synthesis, self-assembly, physical properties, and applications. *Chem. Rev.* **2013**, *113*, 5194−5261.
(23) Srivastava, S.; Agarwal, P.; Archer, L. A. Tethered Nanoparticle-Polymer Composites: Phase Stability and Curvature. *Langmuir* **2012**, *28*, 6276−6281.
(24) Phillips, C. L.; Glotzer, S. C. Effect of nanoparticle polydispersity on the self-assembly of polymer tethered nanospheres. *J. Chem. Phys.* **2012**, *137*, 104901.
(25) Kim, S.; Kim, T.-H.; Huh, J.; Bang, J.; Choi, S.-H. Nanoscale Phase Behavior of Mixed Polymer Ligands on a Gold Nanoparticle Surface. *ACS Macro Lett.* **2015**, *4*, 417−421.
(26) Percebom, A. M.; Giner-Casares, J. J.; Claes, N.; Bals, S.; Loh, W.; Liz-Marzan, L. M. Janus gold nanoparticles obtained via spontaneous binary polymer shell segregation. *Chem. Commun.* **2016**, *52*, 4278−4281.
(27) Li, Y.; Song, L.; Qiao, Y. Spontaneous assembly and synchronous scan spectra of gold nanoparticle monolayer Janus film with thiol-terminated polystyrene. *RSC Adv.* **2014**, *4*, 57611−57614.
(28) Song, L.; Qiao, Y.; Liu, Z.; Li, Y. One-step synthesis of Janus hybrid nanoparticles using reverse atom transfer radical polymerization in emulsion. *Polym. Chem.* **2015**, *6*, 896−899.
(29) Wang, B.; Li, B.; Zhao, B.; Li, C. Y. Amphiphilic Janus gold nanoparticles via combining "solid-state grafting-to" and "grafting-from" methods. *J. Am. Chem. Soc.* **2008**, *130*, 11594−11595.
(30) Lutz, J. F. Thermo-Switchable Materials Prepared Using the OEGMA-Platform. *Adv. Mater.* **2011**, *23*, 2237−2243.
(31) Gil, E. S.; Hudson, S. M. Stimuli-reponsive polymers and their bioconjugates. *Prog. Polym. Sci.* **2004**, *29*, 1173−1222.
(32) Plamper, F. A.; Schmalz, A.; Ballauff, M.; Muller, A. H. E. Tuning the thermoresponsiveness of weak polyelectrolytes by pH and light: Lower and upper critical-solution temperature of Poly(N,N-dimethylaminoethyl methacrylate). *J. Am. Chem. Soc.* **2007**, *129*, 14538−14539.
(33) Glatzel, S.; Laschewsky, A.; Lutz, J.-F. Well-defined uncharged polymers with a sharp UCST in water and in physiological milieu. *Macromolecules* **2011**, *44*, 413−415.
(34) Sugihara, S.; Hashimoto, K.; Okabe, S.; Shibayama, M.; Kanaoka, S.; Aoshima, S. Stimuli-responsive diblock copolymers by living cationic polymerization: Precision synthesis and highly sensitive physical gelation. *Macromolecules* **2004**, *37*, 336−343.
(35) Zarafshani, Z.; Obata, T.; Lutz, J.-F. Smart PEGylation of trypsin. *Biomacromolecules* **2010**, *11*, 2130−2135.
(36) Lavigueur, C.; García, J. G.; Hendriks, L.; Hoogenboom, R.; Cornelissen, J. J.; Nolte, R. J. Thermoresponsive giant biohybrid amphiphiles. *Polym. Chem.* **2011**, *2*, 333−340.
(37) Jones, M. W.; Gibson, M. I.; Mantovani, G.; Haddleton, D. M. Tunable thermo-responsive polymer−protein conjugates via a combination of nucleophilic thiol−ene "click" and SET-LRP. *Polym. Chem.* **2011**, *2*, 572−574.
(38) Ran, F.; Nie, S.; Zhao, W.; Li, J.; Su, B.; Sun, S.; Zhao, C. Biocompatibility of modified polyethersulfone membranes by blending an amphiphilic triblock co-polymer of poly (vinyl pyrrolidone)−b-poly (methyl methacrylate)−b-poly (vinyl pyrrolidone). *Acta Biomater.* **2011**, *7*, 3370−3381.
(39) He, J.; Liu, Y.; Babu, T.; Wei, Z.; Nie, Z. Self-assembly of inorganic nanoparticle vesicles and tubules driven by tethered linear block copolymers. *J. Am. Chem. Soc.* **2012**, *134*, 11342−11345.
(40) Brust, M.; Walker, M.; Bethell, D.; Schiffrin, D. J.; Whyman, R. Synthesis of thiol-derivatised gold nanoparticles in a two-phase liquid−liquid system. *J. Chem. Soc., Chem. Commun.* **1994**, *0*, 801−802.
(41) Xu, L.-P.; Pradhan, S.; Chen, S. Adhesion force studies of Janus nanoparticles. *Langmuir* **2007**, *23*, 8544−8548.
(42) Pradhan, S.; Brown, L. E.; Konopelski, J. P.; Chen, S. Janus nanoparticles: reaction dynamics and NOESY characterization. *J. Nanopart. Res.* **2009**, *11*, 1895−1903.
(43) Pradhan, S.; Xu, L. P.; Chen, S. W. Janus nanoparticles by interfacial engineering. *Adv. Funct. Mater.* **2007**, *17*, 2385−2392.
(44) Ran, F.; Nie, S.; Lu, Y.; Cheng, C.; Wang, D.; Sun, S.; Zhao, C. Comparison of surface segregation and anticoagulant property in block copolymer blended evaporation and phase inversion membranes. *Surf. Interface Anal.* **2012**, *44*, 819−824.
(45) Kalluri, J. R.; Arbneshi, T.; Afrin Khan, S.; Neely, A.; Candice, P.; Varisli, B.; Washington, M.; McAfee, S.; Robinson, B.; Banerjee, S.; et al. Use of gold nanoparticles in a simple colorimetric and

DOI: 10.1021/acs.langmuir.6b00562
Langmuir 2016, 32, 4297−4304

ultrasensitive dynamic light scattering assay: selective detection of arsenic in groundwater. *Angew. Chem.* **2009**, *121*, 9848−9851.

DOI: 10.1021/acs.langmuir.6b00562
Langmuir 2016, 32, 4297−4304

Supporting Information

Thermo-Switchable Janus Gold Nanoparticles with Stimuli-Responsive Hydrophilic Polymer Brushes

Xiaoqin Niu[a], Fen Ran[a,b,*], Limei Chen[a], Gabriella Jia-En Lu[a], Peiguang Hu[a], Christopher P. Deming[a], Yi Peng[a], Mauricio D. Rojas-Andrade[a], and Shaowei Chen[a,*]

[a] *Department of Chemistry and Biochemistry, University of California, 1156 High Street, Santa Cruz, California 95064, USA*
[b] *State Key Laboratory of Advanced Processing and Recycling of Non-ferrous Metals, Lanzhou University of Technology, Lanzhou 730050, P. R. China*
*Corresponding authors: Fen Ran (ranfen@163.com); Shaowei Chen (shaowei@ucsc.edu)

Table S1. Summary of molecular information of the synthesized $PMEO_2MA$-CMTB polymers

Monomer to RAFT agent ratio (wt./wt.)	10:1	30:1	60:1	150:1
M_n ($\times 10^3$)	1.5	4.8	10.2	30.4
M_w/M_n	1.21	1.24	1.25	1.33

Table S2. Summary of FTIR data of the synthesized $PMEO_2MA$ polymers

Peak positions (cm^{-1})	Assignments
2940	Methyl and methylene C–H stretches
2654	S–H stretch
1740	C=O stretch
1456	CH_2 bending
1250	CH_2–O stretch
1144	CH_2–O stretch

Table S3. Summary of FTIR data of the $PMEO_2MA$-tethered gold Janus nanoparticles

Peak positions (cm^{-1})	Assignments
2940	Methyl and methylene C–H stretches
1740	C=O stretch
1250	CH_2–O stretch